Indian J. Phys. **47**, 681–692 (1973)

Effect of strong blowing on conducting flow between a sliding and a stationary cylinder

B. C. CHANDRASEKHARA, S. B. LALSANGI* AND N. RUDRAIAH

Department of Mathematics (Post-Graduate Studies)
Visvesvarya College of Engineering, Bangalore University
Bangalore-1, India

(*Received* 26 *July* 1972, *revised* 24 *October* 1972)

The effect of strong blowing on a conducting flow between a sliding and a stationary cylinder is examined in the presence of a variable radial magnetic field and variable injection velocities. Closed-form solutions are obtained for the problem including heat transfer, gravity and both axial and radial pressure gradients In the massive blowing regime the asymptotic solution possesses two-layered structure whose nature depends on orientation of the system and the axial pressure gradient. The results of the analysis show that the shear layer blow off from the blown surface occurs for large values of injection Reynolds number and Hartmann number

NOMENCLATURE

B magnetic induction vector
B_1 variable magnetic induction
B^* non dimensional reference magnetic induction
E electric field vector
E_θ azimuthal component of electric field
F Froude number, v_w^2/gh
g nondimensional enthalpy, $(H-H_1)/(H_0-H_1)$
H magnetic field vector
H_x^* induced magnetic field in the axial direction
h gap between the two cylinders
K thermal conductivity
J current density vector
M Hartmann number, $\{(\sigma A^2 h^2)/(\rho \nu r_1^2)\}^{\frac{1}{2}}$
N square of the ratio of velocities, U^2/v_w^2
P nondimensional pressure, $P_0/\rho v_w^2$
p pressure
P_0 atmospheric pressure
P_r Prandtl number, ν/K
R Reynolds number based on sliding velocity, Uh/ν
R_b injection Reynolds number, $v_w h/\nu$
R_m magnetic Reynolds number, $\mu\sigma Uh$
r radial coordinate
r_0 radius of the outer cylinder
r_1 radius of the inner cylinder
U sliding velocity
v_w injection velocity at the inner cylinder
v_e injection velocity at the outer cylinder

* K.L.E. Society's S. Nijalingappa College, Bangalore-10.

u^* nondimensional sliding velocity, u/U
v_w^* nondimensional injection velocity, v/v_w
V velocity vector
z inner variable
ρ density of the fluid
ν kinematic viscosity
μ_f absolute viscosity of the fluid
μ magnetic permeability
σ electrical conductivity of the fluid
η nondimensional radial coordinate, $(r-r_i)/(r_0-r_i)$
λ transverse curvature parameter, h/r_i
Λ nondimensional axial pressure gradient parameter, $\frac{h^2 dp/dx}{\rho\nu U}$
ϵ nondimensional parameter, R/NF
θ inclination of the system with the horizontal

Introduction

The study of the effect of strong blowing on flow fields is of considerable interest in aerodynamics and has been examined by a number of investigators (White *et al* 1958, Yuan & Finkelstein 1956, Terrill 1955, 1964, Rasmussen 1970). Specifically, the strong blowing of mass into the boundary layer has long been considered as a possible means of protection of the noses of reentry vehicles from high heat fluxes(Barber 1965). In recent year the mass addition has also taken many forms including transpiration cooling, mass transfer cooling and film cooling These three models have been reviewed by Rudraiah (1966). An experimental investigation of fluid injection at the stagnation point has been made by Barber and this has shown that there exists three regimes of flow interaction namely, boundary-layer regime, viscous regime and shock regime Similar studies, describing some of the major physical features involved in the interaction of blowing with a shear layer, have been previously made, considering simplified flow model like Couette-Poiseuille shear flows (Cramer 1959, Inman 1959, Lilley 1959, Artzukh & Kashkarov 1966). Recently Inger (1969) has re-examined the above problem including the presence of heat transfer and both axial and radial pressure gradients. In particular, he has emphasized the behaviour of the solution in the strong blowing regime He finds that shear layer blow-off from the blown surface occurs for sufficiently strong injection and the flow in this asymptotic regime has two-layered structure, whose basic character depends critically on whether or not an axial pressure graident is present. In magnetohydrodynamics the effect of strong belowing on conducting flows has been investigated by Shrestha (1967), Rudraiah & Chandrasekhara (1969) for different physical situations and different geometrical configurations. These investigations pertain to the study of the effect of injection on the boundary layer. The strong blowing of a conducting fluid into space-craft body in the presence of a solar magnetic field, is of particular interest in the space research problems. In laboratory this problem is also of particular interest in the design of MHD slider bearing system. These problems

are mathematically complicated in realistic flow configurations In such circumstances, a simple flow model is ideal to understand some of the major physical features involved in the interaction of blowing with a conducting shear layer and magnetic field. An ideal model for this purpose is the well-known Couette-Hartmann shear flow since the solution of this problem can be expressed in closed form and it possesses a qualitative similarity to Hatmann boundary layer type of flows including the total pressure (*i.e* , the sum of the hydrostatic and magnetic pressure) gradient effects. This problem with inertia and viscous effects and with strong blowing has not been given much attention in magnetohydrodynamics. Therefore, the aim of the present discussion is to study the interaction of strong blowing on the forced convective flow of conducting fluid, between a sliding and a stationary cylinder, oriented at different angles to the horizontal. The results of this analysis emphasize the behaviour of the solution in the strong blowing regime and the solution is obtained in the unified form applicable to both two-dimensional and axi-symmetric flows

Formulation of the problem

A uniform incompressible conducting fluid of density ρ, viscosity μ_f and electrical conductivity σ flows through an annular channel formed by two infinitely long porous concentric cylinders of radii r_0 and r_i. The outer cylinder r_0 slides with an uniform axial velocity $u = U$ relative to the stationary inner cylinder. The fluid is injected radially with uniform velocity v through the inner cylinder and due to the conservation of mass, the fluid also flows outward through the sliding cylinder with some radial velocity v_e. An external variable magnetic field of the form $B_r = A/r$ is applied in the radial direction (figure 1) (The generation of such a magnetic field in the laboratory has been suggested by Globe 1959). The flow is axisymmetric and we are considering the variable injection velocity (*i.e.*, $v = c/r$) in the radial direction, the equations of continuity of fluid and magnetic field $\Delta.V = 0 = \Delta.B$ show that all the physical quantities of the flow are functions of r only save for pressure which may have an arbitrary constant axial pressure gradient

Defining the normalized distance $\eta = (r-r_i)/(r_0-r_i)$ and a transversecurvature parameter $\lambda = h/r_i$ such that $(r/r_i) = 1+\lambda\eta$, the axi-symmetric three dimen-

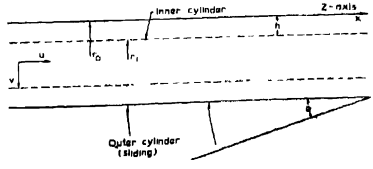

Figure 1. Physical model.

sional problem reduces to two-dimentional case in the limit $\lambda \to 0$ The governing equations of motion, introducing the dimensionless velocity, pressure, magnetic field and enthalpy variables

$$u^* = \frac{u}{U}, \quad v^* = \frac{v}{V_\omega}, \quad P = \frac{p}{\rho v_\omega^2}$$

$$B^* = \frac{B}{A\sqrt{h}}, \quad g = \frac{H-H_i}{H_0-H_i}, \quad H = h+\tfrac{1}{2}u^2$$

into the Navier-Stokes equations and the energy equation are

$$(1+\lambda\eta)v^* = 1, \qquad \ldots (1)$$

$$R_b \frac{du^*}{d\eta} = \frac{d}{d\eta}\left\{(1+\lambda\eta)\frac{du^*}{d\eta}\right\} - (\Lambda - \epsilon \sin\theta)(1+\lambda\eta) - \frac{M^2 u^*}{1+\lambda\eta}, \qquad \ldots (2)$$

$$v^* \frac{dv^*}{d\eta} = -\frac{dP}{d\eta} + \frac{M^2 N u^* H_x^*}{\lambda(1+\lambda\eta)} + \frac{\cos\theta}{F}, \qquad \ldots (3)$$

$$P_r R_b \frac{dg}{d\eta} - \frac{d}{d\eta}\left\{(1+\lambda\eta)\frac{dg}{d\eta}\right\} = \frac{P_r v_\omega^2 \lambda (1+\lambda\eta)^{-3}}{H_0-H_i}\left(R_b + \tfrac{4}{3}\lambda\right) + \frac{v_\omega^2 P_r}{H_0-H_i}\cdot\frac{\cos\theta}{F} + \frac{v_\omega^2 P_r M^2 N^2 u^{*2}}{\lambda^2(H_0-H_i)}(1+\lambda\eta)^{-1} \qquad \ldots (4)$$

The boundary conditions are

$$u^*(0) = g(0) = 0, \qquad u^*(1) = g(1) = 1$$

$$v^*(0) = 1, \qquad v^*(1) = 1/1+\lambda$$

and these give $P(1) = P_0/\rho v^2{}_w$

The momentum equation (3) has purely an inviscid character even in the presence of magnetic field and gravitational force because of the nature of the injection velocity $v^* = 1/1+\lambda\eta$. Since we are dealing with practically forced convection problem, where the velocities involved are not small, we have included the ohmic and viscous dissipation effects in the energy equation (4). In the hydrodynamic case of Inger (1969), dissipation of energy is mainly because of the radial shear stress and the normal pressure However, in the present magneto-hydrodynamic case in addition to these dissipations we have ohmic dissipation. In the absence of blowing and transverse curvature, dissipation term arises entirely due to ohmic heating in equation (4)

Pressure distribution

Examining equation (3) we find that the radial pressure change is brought about due to induced and applied magnetic fields, gravity and the momentum

change associated with the turning of the injected fluid. Since the induced magnetic field term, is involved in equation (3), we should calculate the induced magnetic field H_x^* before integrating equation (3). The equation for H_x^*, is obtained from the magnetic induction equation under the assumption of small R_m, in the form

$$-R_m \frac{du^*}{d\eta} = \left(\frac{1+\lambda\eta}{\lambda}\right) \frac{d^2H_x^*}{d\eta^2} + \frac{dH_x^*}{d\eta} \qquad \ldots (5)$$

The boundary conditions on H_x^* are

$$H_x^*(1) = 0, \qquad \frac{dH_x^*}{d\eta}(1) = -\frac{R_m\lambda}{1+\lambda} \qquad \ldots (6)$$

The above boundary conditions are obtained as follows The current density J has only θ component, so that the current in the annular channel is analogous to that in an infinite solenoid and may be assumed to produce no field for $\eta > 1$. Thus the continuity of tangential component of magnetic field requires that $H_x^*(1) = 0$. The remaining boundary condition is obtained by assuming that the walls of the cylinders are perfect conductors and hence the tangential component of the electric field E_θ will be zero at the walls From

$$J = \sigma(E+\mu V \times H) = \nabla \times H$$

and using equation (5) we obtain

$$\frac{dH_x^*}{d\eta}(1) = -R_m\lambda/1+\lambda \qquad \ldots (7)$$

Solving equation (6) for H_x^* and then substituting it in equation (3) and integrating we obtain an expression for P_0-P. Since the expression for P_0-P is complicated we have presented non-dimensional pressure profiles in figure (2).

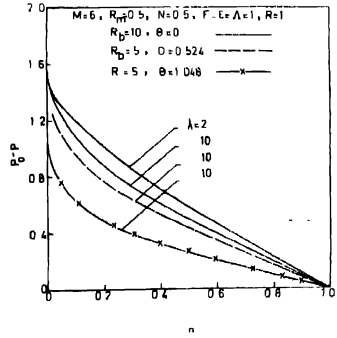

Figure 2. Pressure distribution across the channel.

From figure (2) we find that in the absence of magnetic field and $\theta = 0$. the magnitude of the pressure is nearly 50 percent greater compared to Inger's profiles This increase in pressure is entirely due to gravity and we note that as θ increases there is considerable reduction in pressure. However, increase in transverse curvature parameter λ, for a given angle of orientation, reduces the pressure slightly. We also note that there is a slight increase in pressure for a given M and different R_b and similar trend is observed as M and N are increased for a given R_b. The overall pressure-rise, in all these situations, is evenly distributed across the channel for all values of λ.

Velocity distribution

The expression for the axial velocity u^*, obtained by solving the momentum equation (2), using the boundary conditions (5), is

$$u^* = \left[1 - \left(\frac{\Lambda - \epsilon \sin\theta}{S} \right) \frac{\{(1+\lambda)^2 - (1+\lambda)^{\lambda_2/\lambda}\}}{(1+\lambda)^{\lambda_1/\lambda} - (1+\lambda)^{\lambda_2/\lambda}} \right] \left\{ (1+\lambda\eta)^{\lambda_1/\lambda} - (1+\lambda\eta)^{\lambda_2/\lambda} \right\} +$$

$$+ \left(\frac{\Lambda - \epsilon \sin\theta}{S} \right) \left\{ (1+\lambda\eta)^2 - (1+\lambda\eta)^{\lambda_2/\lambda} \right\} \qquad \ldots (8)$$

and the axial shear stress at the inner cylinder is

$$\left(\frac{du^*}{d\eta} \right)_{\eta=0} = - \left(\frac{\Lambda - c \sin\theta}{S} \right) \left\{ (1+\lambda)^2 - (1+\lambda)^{\lambda_2/\lambda} \right\} \left\{ \frac{\lambda_1 - \lambda_2}{(1+\lambda)^{\lambda_1/\lambda} - (1+\lambda)^{\lambda_2/\lambda}} \right\}$$

$$+ \frac{\Lambda - \epsilon \sin\theta}{S} (2\lambda - \lambda_2), \qquad \ldots (9)$$

where $\lambda_1 = \dfrac{R_b + (R_b^2 + 4M^2)^{\frac{1}{2}}}{2}$, $\lambda_2 = \dfrac{R_b - (R_b^2 + 4M^2)^{\frac{1}{2}}}{2}$,

$$(\lambda_1 < 0, \quad \lambda_2 < 0) \quad \text{and} \quad S = 4\lambda^2 - 2R_b\,\lambda - M^2$$

We note that equation (8) reduces to the two-dimensional case in the limit $\lambda \to 0$ and it is in the form

$$u^*_{\lambda \to 0} = \left[\frac{1 + \dfrac{\Lambda - \epsilon \sin\theta}{M^2} \{1 + \exp \lambda_2\}}{\exp \lambda_1 - \exp \lambda_2} \right] \{\exp \lambda_1\eta - \exp \lambda_2\eta\} -$$

$$- \frac{\Lambda - \epsilon \sin\theta}{M^2} (1 - \exp \lambda_2\eta) \qquad \ldots (10)$$

Equation (10) reduces to the Hydrodynamic result of Inger (1969) in the limit $M \to 0$ when $\theta = 0$,

$$i.e. \qquad u^*_{\lambda \to 0} = \left\{1 + \frac{\lambda}{R_b}\right\}\left\{\frac{\exp R_b\eta - 1}{\exp R_b - 1}\right\} - \frac{\Lambda\eta}{R_b} \qquad \ldots (11)$$

Some typical velocity profiles are presented in figures 3, 4 and 5 for zero axial pressure gradient. We find that the velocity profiles (figure 3) are similar in nature to the velocity profiles in the hydrodynamic case The combined effect of magnetic field and blowing for small values of the transverse curvature parameter is to reduce the magnitude of the velocity and push the boundary layer towards the rigid boundaries. However, for large values of the transverse curvature parameter the combined effect of magnetic field and blowing is to increase the

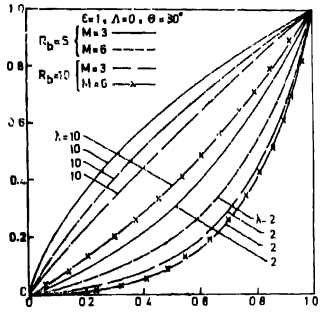

Figure 3, Typical axial velocity profiles.

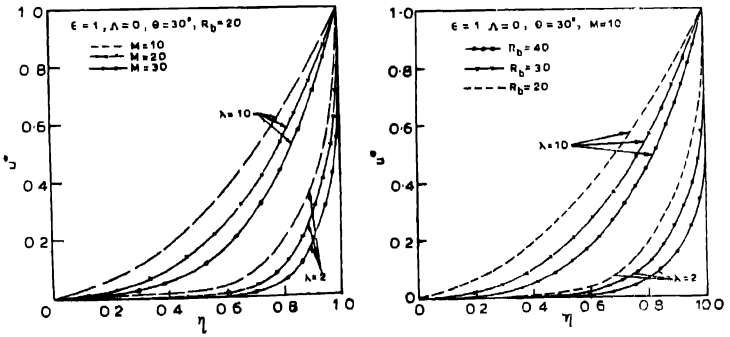

Figure 3a, 3b, Typical axial velocity profiles.

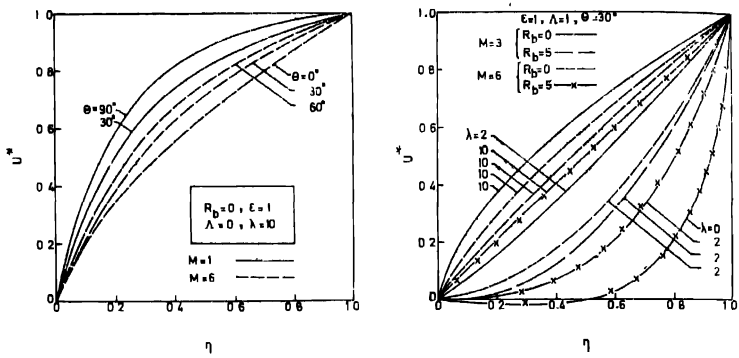

Figure 4, 5. Typical axial velocity profiles

magnitude of the velocity and flatten the velocity profiles. Figure 3a shows the effect of large values of magnetic field on the velocity distribution for a given value of R_b. It is observed that the velocity profiles are flattened and the boundary layer is pushed towards the rigid boundaries which is analogous to that of suction. Figure 3b shows the effect of large blowing on the velocity distribution. It is seen that in the presence of magnetic field the velocity profiles are flattened even in the case of large blowing which is due to the fact that the magnetic field generates electric current which retards the flow. Figure 4 shows the effect of angle of orientation on the velocity distribution in the absence of blowing. It is observed that increase in the angle of orientation increases the velocity, whereas, increase in magnetic field for a given angle of orientation reduces the velocity. In the case of adverse pressure gradient (figure 5) the solution exhibits the flow reversal for $\lambda = 0$ under the action of strong blowing even in the presence of magnetic field. The critical value of Λ for separation $(du^*/d\eta)_{\eta=0} = 0$ is obtained from equation (9) in the form

$$\Lambda_{sep} = \frac{\left(\frac{\lambda_1-\lambda_2}{\lambda}\right) S+\epsilon \sin\theta \left[\left\{(1+\lambda)^2-(1+\lambda)^{\lambda_2/\lambda}\right\}\left(\frac{\lambda_1-\lambda_2}{\lambda}\right) - \left(2-\frac{\lambda_2}{\lambda}\right)\left\{(1+\lambda)^{\lambda_1/\lambda}-(1+\lambda)^{\lambda_2/\lambda}\right\}\right]}{\left\{(1+\lambda)^2-(1+\lambda)^{\lambda_2/\lambda}\right\}\frac{\lambda_1-\lambda_2}{\lambda}-\left(2-\frac{\lambda_2}{\lambda}\right)\left\{(1+\lambda)^{\lambda_1/\lambda}-(1+\lambda)^{\lambda_2/\lambda}\right\}} \quad (12)$$

This is plotted in figure 6 and we observe that the effect of blowing is to decrease Λ_{sep}. We also observe that under very strong blowing conditions, flow reversal is caused by small adverse pressure gradients when $\theta = 0$. However, Λ_{sep} approaches asymptotically to a definite value when $\theta < 0$. For a given value of M, increase in λ increases Λ_{sep}; whereas, for a given value of λ increase in M

reduces the value of Λ_{sep}. Thus both transverse curvature and favourable pressure gradient ($\Lambda < 0$) intensity the inner surface shear $(du^*/d\eta)_{\eta=0}$, while magnetic field and blowing tend to reduce it.

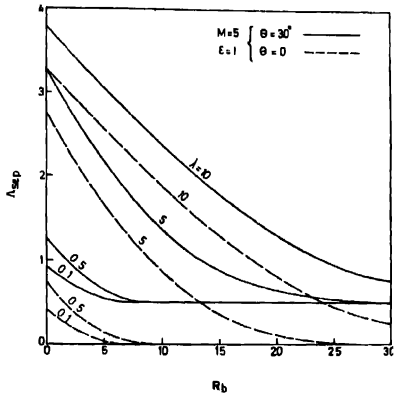

Figure 6. Axial pressure gradient variation for different values of Λ.

We now study the structure of the solutions (8) in the massive blowing limit $R_b \gg 1$ for a given λ. Appropriate to this limit equations (8) and (9) excluding the case $\lambda \gtrsim 0(R_b)$, can be written in the following approximate forms;

$$u^* \simeq \left[1+\frac{(\Lambda-\epsilon\sin\theta)(2+\lambda)}{2R_b+M^2/\lambda}\right]\left[\exp\left(-\frac{\lambda_1}{\lambda}\log\frac{1+\lambda}{1+\lambda\eta}\right)-\exp\left(-\frac{\lambda_1}{\lambda}\log(1+\lambda)\right)\right]$$

$$-\frac{\eta(2+\lambda\eta)(\Lambda-\epsilon\sin\theta)}{2R_b+M^2/\lambda}, \qquad \ldots (13)$$

$$\left(\frac{du^*}{d\eta}\right)_{\eta=0} \simeq \left[1+\frac{(\Lambda-\epsilon\sin\theta)(2+\lambda)}{2R_b+M^2/\lambda}\right]\lambda_1\exp\left\{-\frac{\lambda_1}{\lambda}\log(1+\lambda)\right\}-\frac{2(\Lambda-\epsilon\sin\theta)}{2R_b+M^2/\lambda}, \qquad \ldots (14)$$

$$\left(\frac{du^*}{d\eta}\right)_{\eta=1} \simeq \left[1+\frac{(\Lambda-\epsilon\sin\theta)}{2R_b+M^2/\lambda}\right]\frac{\lambda_1}{\lambda}-\frac{2(1+\lambda)(\Lambda-\epsilon\sin\theta)}{2R_b+M^2/\lambda}, \qquad \ldots (15)$$

When $M = 0$, we have

$$\left(\frac{du^*}{d\eta}\right)_{\eta=0} \simeq \left[R_b+\frac{(2+\lambda)\Lambda}{2}\right]\exp\left(-\frac{R}{\lambda}\log(1+\lambda)\right)-\frac{\Lambda}{R_b}, \qquad \ldots (16)$$

$$\left(\frac{du^*}{d\eta}\right)_{\eta=1} \simeq \left[1+\frac{\Lambda(2+\lambda)}{2R_b}\right]\frac{R_b}{1+\lambda}-\frac{\Lambda(1+\lambda)}{R_b}, \qquad \ldots (17)$$

where the terms of the order λ/R_b^2 and higher are neglected. These relations (13) and (14), show that the wall shear and axial velocity over some distance from the stationary cylinder tend to vanish for large values of R_b and M, suggesting that the shear layer becomes effectively blown off the surface. Further at the moving cylinder (*i.e.* $\eta = 1$) the shear stress increases with increase in R_b and M for a given λ. We find, comparing with the hydrodynamic results, that the effect of magnetic field is to increase the shear stress in the inner shear layer A close examination of this asymptotic solution reveals that this solution possesses two-layered structure, whose nature depends on R_b and the axial pressure gradient

We can identify an outer solution in each of these equations (13) and (24), which is valid in the entire flow region except for small thin region near the moving surface, since the first term on the right side of these equations is exponentially small for sufficintly large values of R_b and M When $\Lambda = 0$ and $\theta = 0$ this outer solution for u^* is exponentially small and all of its derivatives vanish to any algebric order in R_b and M. However, if $\Lambda \neq 0$ or $\theta > 0$ the outer solution becomes a constant shear motion which depends algebraically on the blowing rate and the magnetic field This type of motion is qualitatively similar to MHD laminar flows under the action of large injection, in a uniformly porous channel and between porous disks studied by Shrestha (1967), Rudaiah & Chandrasekhara (1969) The inner solution which is valid in the thin region near the moving surface is obtained by introducing an inner variable $z = (\lambda_1/\lambda) \log (1+\lambda)/(1+\lambda\eta)$ into equation (13) and it takes the form

$$u^* \simeq e^{-z} + \frac{(2+\lambda)(\Lambda - \epsilon \sin\theta)}{2R_b + M^2/\lambda} \left\{ e^{-z} - 1 \right\} + 0(\lambda_1^{-2}) , \qquad .. \quad (18)$$

where $z(\eta = 1) = 0, z(\eta = 0) = \infty$. This inner solution has a completely algebraic dependence on R_b and M for all values of Λ and is independent of Λ in the leading asymptotic expansion In fact equation (18) is the complete asymptotic massive blowing solution throughout the flow region when $\Lambda = 0$ and $\theta = 0$, for the leading term satisfies both the bounday conditions $u^*(z = 0) = 1$ and $u^*(z = \infty) = 0$ When $\Lambda \leqslant 0$ or $\theta > 0$ this is no longer true and the full solution now consists of the inner solution (18) properly matched to the constant shear outer solution These conclusions are qualitatively illustrated in figures 7(*a*) and 7(*b*).

Energy Equation

Since the expression for enthalpy is complicated we have not given the expression however it is numerically evaluated and some typical non-dimensional enthalpy profiles are presented in figure (8). These profiles, in general, are similar in shape and physical trends to the velocity profiles We find that increase in λ increases the heat transfer while increase in R_b reduces the heat transfer. We

also note that the effect of increase in M and θ is to reduce the heat transfer while other parameters remain constant

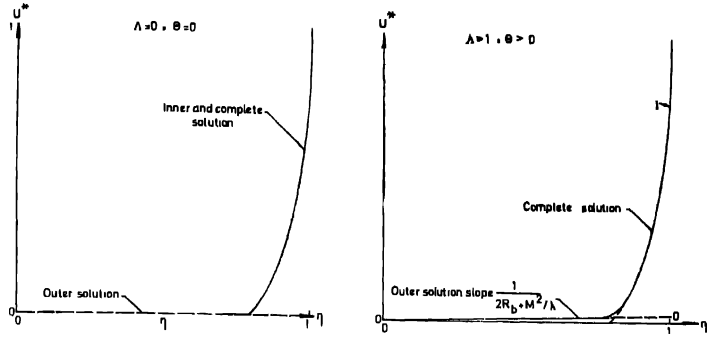

Figure 7(a), 7(b) Schematic of asymptotic massive blowing solution.

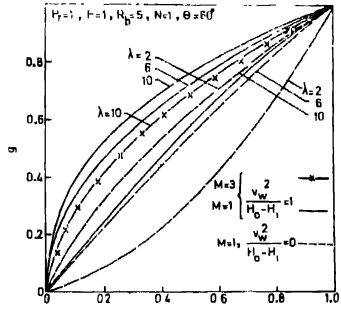

Figure 8. Total enthalpy profiles.

Conclusions

In the present analysis we have considered an idealized simple model of MHD Couette-Hartmann shear flow to investigate the effect of massive blowing in the presence of a radial variable magnetic field for different orientations of the physical model. This model in fact exhibits all the physical characteristics associated with injection of fluid to the boundary layer flows In addition to the above characteristics some of the important features like the existence of two-layered structure of the solution are also identified in the massive blowing regime. In

the massive blowing regime the solution exhibits a singular behaviour when the axial pressure gradient is zero and $\theta = 0$ and the inner solution alone is a complete solution. However, when $\Lambda \leqslant 0$ and $\theta > 0$ the complete solution consists of a constant shear outer region which depends on R_b and M, properly matched to an inner solution which is associated with a thin region near the moving surface. The overall effect of the magnetic field and the inclination θ is to push the point of maximum velocity gradient towards the stationary disk, to increase the pressure and to reduce the heat transfer at the walls. Thus our results are of some use in the transpiration cooling devices which are commonly used in the space research problems. We also conclude that since the gravity and the magnetic field increases the pressure, results are of some help in the design of MHD porous slider bearing in the sense that the radial injection of the fluid, the gravity and the magnetic field increase the lubrication effect by effectively pumping the fluid between the bearing surfaces.

ACKNOWLEDGEMENT

We thank the referee for his many valuable suggestions and comments.

REFERENCES

Artzukh L. Y. & Kashkarov V P. 1966 *Intern J. Heat Mass Transfer*. **9**, 1075.
Barber F. A. J. 1965 *J. Space-Craft Rockets* **2**, 770.
Cramer K. R. 1959 *J. Aerospace. Sci* **26**, 121.
Dunwoody N. T. 1962 *J. Aerospace Sci.* **29**, 404
Globe S. 1959 *Phy. Fluids* **2**, 404.
Inger G. R. 1969 *Phys. Fluids*. **12**, 1741.
Inman R. M. 1959 *J. Aerospace Sci* **26**, 532.
Lilley G. M. 1959 *J. Aerospace Sci.* **26**, 685
Rasmussen H. 1970 *ZAMP* **21**, 178.
Rudraiah N. 1966 *Technical note. TN-PH-4-66 NAL*, Banalore.
Rudraiah N. & Chandrasekhara B. C. 1969 *Bull. Aca Sci. Georgian SSR* **53**, 285.
Shrestha G. M. 1967 *QJMAM* **20**, 233.
Terrill R. M. 1955 *Aeronaut. Quart.* **16**, 323.
Terrill R. M. 1964 *Aeronaut Quart.* **15**, 299.
White F. M Jr., Barfield & Gogila M. J. 1958 *J. Appl Mech.* **25**, 613.
Yuan S. W. & Finkelstein A. B. 1956 *Trans. ASME* **72**, 719.